Blocking rpS6 Phosphorylation Exacerbates *Tsc1* Deletion–Induced Kidney Growth

Huijuan Wu,*† Jianchun Chen,‡ Jinxian Xu,*† Zheng Dong,*§ Oded Meyuhas,‖ and Jian-Kang Chen*†

*Department of Cellular Biology and Anatomy, †Department of Medicine, Medical College of Georgia, Georgia Regents University, Augusta, Georgia; ‡Division of Nephrology and Hypertension, Department of Medicine, Vanderbilt University School of Medicine, Nashville, Tennessee; §Research Department, Charlie Norwood VA Medical Center, Augusta, Georgia; and ‖Department of Biochemistry and Molecular Biology, Institute for Medical Research Israel–Canada, Hebrew University Hadassah Medical School, Jerusalem, Israel

ABSTRACT

The molecular mechanisms underlying renal growth and renal growth–induced nephron damage remain poorly understood. Here, we report that in murine models, deletion of the tuberous sclerosis complex protein 1 (Tsc1) in renal proximal tubules induced strikingly enlarged kidneys, with minimal cystogenesis and occasional microscopic tumorigenesis. Signaling studies revealed hyperphosphorylation of eukaryotic translation initiation factor 4E-binding protein 1 (4E-BP1) and increased phosphorylation of ribosomal protein S6 (rpS6) in activated renal tubules. Notably, knockin of a nonphosphorylatable rpS6 in these *Tsc1*-mutant mice exacerbated cystogenesis and caused drastic nephron damage and renal fibrosis, leading to kidney failure and a premature death rate of 67% by 9 weeks of age. In contrast, *Tsc1* single-mutant mice were all alive and had far fewer renal cysts at this age. Mechanistic studies revealed persistent activation of mammalian target of rapamycin complex 1 (mTORC1) signaling causing hyperphosphorylation and consequent accumulation of 4E-BP1, along with greater cell proliferation, in the renal tubules of *Tsc1* and *rpS6* double-mutant mice. Furthermore, pharmacologic treatment of *Tsc1* single-mutant mice with rapamycin reduced hyperphosphorylation and accumulation of 4E-BP1 but also inhibited phosphorylation of rpS6. Rapamycin also exacerbated cystic and fibrotic lesions and impaired kidney function in these mice, consequently leading to a premature death rate of 40% within 2 weeks of treatment, despite destroying tumors and decreasing kidney size. These findings indicate that Tsc1 prevents aberrant renal growth and tumorigenesis by inhibiting mTORC1 signaling, whereas phosphorylated rpS6 suppresses cystogenesis and fibrosis in *Tsc1*-deleted kidneys.

J Am Soc Nephrol 27: 1145–1158, 2016. doi: 10.1681/ASN.2014121264

Reduction in the number of functional nephrons stimulates the residual functioning nephrons to undergo compensatory growth. It is recognized that compensatory renal growth occurs not only after surgical renal ablation (due to renal trauma or tumor) but also occurs in virtually all kidney diseases that cause nephron damage and consequently a reduction in functioning nephron number.[1–4] However, excessive renal growth may be a maladaptive response and has been implicated in progressive nephron damage, leading to ESRD.[2–6]

The mammalian target of rapamycin (mTOR) is an evolutionarily conserved serine/threonine protein kinase that regulates protein synthesis, cell growth, and proliferation by integrating multiple environmental and intracellular cues, including

Received December 24, 2014. Accepted July 16, 2015.

Published online ahead of print. Publication date available at www.jasn.org.

Present address: Dr. Huijuan Wu, Department of Pathology, School of Basic Medical Sciences, Fudan University, Shanghai, China.

Correspondence: Dr. Jian-Kang Chen, Department of Cellular Biology & Anatomy, Department of Medicine, Medical College of Georgia, Georgia Regents University, 1459 Laney Walker Boulevard, CB2200, Augusta, GA 30912. Email: jchen@gru.edu

growth factors, nutrients, energy status, oxygen and stress levels.[7,8] mTOR forms two structurally and functionally distinct multiprotein complexes: mTOR complex 1 (mTORC1) and mTORC2 in all mammalian cells.[7] The regulatory-associated protein of mTOR (Raptor) only exists in mTORC1 while the rapamycin-insensitive companion of mTOR (Rictor) is the key component of mTORC2. mTORC1 functions largely through phosphorylation of two downstream targets: the ribosomal protein S6 kinase 1 (S6K1) and eukaryotic translation initiation factor 4E-binding protein 1 (4E-BP1). mTORC1 phosphorylates and inhibits 4E-BP1; meanwhile it phosphorylates S6K1 at T389 to activate S6K1, which further phosphorylates multiple downstream targets, including the ribosomal protein S6 (rpS6).[9–12] Unlike mTORC1, mTORC2 does not regulate the phosphorylation of 4E-BP1 or S6K1.[13]

For a cell to grow in size or to proliferate, a positive signal is required to drive increased protein synthesis in the cell. In this regard, we initially observed that mTORC1 activation is a positive signal that mediates increased protein synthesis during uninephrectomy-induced renal growth,[14] and our further studies identified increased amino acids (delivered into the remaining kidney by increased renal blood flow in response to uninephrectomy) as molecular growth signals that initiate mTORC1 activation.[15] In a previous study, Bell *et al.* hypothesized that primary cilia prevent renal cyst formation by suppressing pathologic tubular cell hypertrophy and proliferation, with the primary purpose of determining if hypertrophic signaling could modify the rate of cystogenesis.[16] Their results demonstrated that uninephrectomy induced mTORC1 signaling and renal hypertrophy without cyst formation in wild-type (WT) mice; however, uninephrectomy activated excessive mTORC1 signaling, triggered increased renal hypertrophy and accelerated renal cyst formation, leading to renal dysfunction in conditional *ift88* knockout mice.[16] Of interest, mTORC1 activation also mediates both diabetes-induced renal growth[17–19] and phosphatase and tensin homolog deletion-induced renal growth.[15] Homozygous knockout of S6K1 blunts both uninephrectomy- and diabetes-induced renal growth,[17] and phosphorylated rpS6 is a major effector downstream of mTORC1 activation in mediating compensatory renal growth.[20] Therefore, we hypothesize that mTORC1 is a master regulator that controls kidney size and mTORC1 activation is a "common

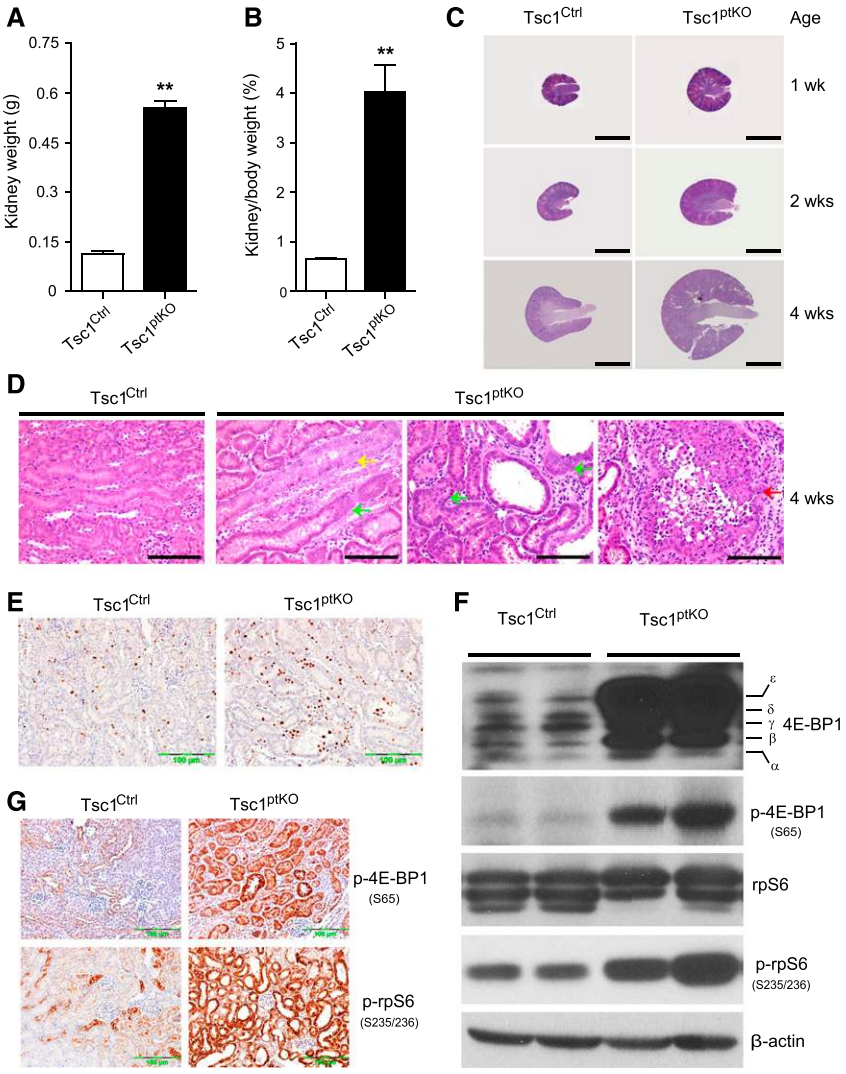

Figure 1. Characterization of renal proximal tubule cell-specific Tsc1 knockout ($Tsc1^{ptKO}$) mice. (A, B) $Tsc1^{ptKO}$ mice (n=6) had significantly increased (A) kidney weights and (B) kidney to body weight ratios, compared with their $Tsc1^{Ctrl}$ littermates (n=5). Data were from mice at 6 weeks of age and expressed as means±SEM, $^{**}P<0.01$. (C) Representative whole kidney sections with H&E staining from $Tsc1^{ptKO}$ and $Tsc1^{Ctrl}$ mice at 1, 2, and 4 weeks of age, with $Tsc1^{ptKO}$ mice showing increased kidney size. (D) Higher magnification light microscopy revealed markedly enlarged renal proximal tubules lined with hyperplastic (green arrows) and hypertrophic epithelial cells (yellow arrow), with a few microscopic renal cysts and occasional renal tumors (red arrow) in $Tsc1^{ptKO}$ mice, compared $Tsc1^{Ctrl}$ mice. (E) Immunohistochemical staining with an antibody specific for the proliferating cell marker Ki67 revealed markedly increased cell proliferation in $Tsc1^{ptKO}$ kidneys. (F) Immunoblotting of kidney cortex homogenates indicated aberrantly upregulated protein expression of total 4E-BP1 and phosphorylation of both 4E-BP1 and rpS6 in $Tsc1^{ptKO}$ kidneys. (G) Immunohistochemical staining localized the increased p-rpS6 and p-4E-BP1 to the epithelial cells of activated renal tubules in $Tsc1^{ptKO}$ mice. Representative blots shown were from at least three separate experiments with similar results. (Scale bars: 2 mm in all images of C; 100 μm in all images of D, E, and G.)

denominator" leading to renal growth, although the initiating growth stimuli in different situations may not be the same.

The tuberous sclerosis complex protein 1 (Tsc1) is considered a negative regulator of mTORC1,[8] and renal proximal tubules make up the bulk of the kidney.[21,22] So we tested the hypothesis that selectively deleting Tsc1 in proximal tubules would be sufficient to activate mTORC1 and induce kidney growth. In addition, mTORC1 activation is implicated in the genetic disorder known as tuberous sclerosis complex, caused by gene mutations in either *TSC1* or *TSC2* (the human homologs of mouse *Tsc1* and *Tsc2* genes, respectively).[23,24] However, mTOR has multiple substrates,[25,26] which might underlie the many adverse effects of the clinically used mTOR inhibitors.[27] So in the present study, we also tested the hypothesis that selectively blocking only rpS6 phosphorylation might provide proof-of-concept evidence for the development of an improved new therapy to prevent renal growth-induced nephron damage, given that rpS6 phosphorylation is implicated in cell growth and proliferation.[20,28–30]

RESULTS

Tsc1 Deletion in Renal Proximal Tubules Caused Striking Kidney Growth

By crossing *Tsc1*-floxed mice (*Tsc1*$^{flox/flox}$) with transgenic mice expressing Cre recombinase under the control of the gamma glutamyl transpeptidase (γGT) promoter,[31] we generated a new line of proximal tubule-specific *Tsc1* gene knockout (Tsc1^{ptKO}) mice, as illustrated in Supplemental Figure 1A. Gender-matched *Tsc1*$^{flox/flox}$; *γGT-Cre*$^{-}$ littermates were used as control mice (called Tsc1^{Ctrl} mice hereafter). PCR genotyping identified Tsc1^{Ctrl} and Tsc1^{ptKO} mice as those carrying only *Tsc1*-floxed alleles, while the heterozygous floxed (Tsc1^{Hets}) mice harbored both the *Tsc1*-floxed allele and the WT allele; however, the *γGT-Cre* gene was only detected in Tsc1^{ptKO} mice (Supplemental Figure 1B). Immunoblotting of proximal tubule-enriched renal cortex homogenates confirmed effective deletion of Tsc1 protein (Supplemental Figure 1C).

Tsc1^{ptKO} mice showed significantly increased kidney weights (Figure 1A) and kidney to body weight ratios (Figure 1B), with strikingly increased kidney size (Figures 1C and 4C). The large kidney phenotype was caused by both cellular hypertrophy and cell proliferation, which led to markedly enlarged proximal tubules (some tubules were aberrantly lined with multiple layers of proliferating cells), with some small renal cysts (Figure 1D). Immunohistochemical staining for Ki67, a marker for proliferating cells, confirmed markedly increased cell proliferation (Figure 1E). By 4 weeks of age, Tsc1^{ptKO} mice developed occasional microscopic tumors, seemingly resulting from dysregulated tubular epithelial cell proliferation filling up the lumens of enlarged renal tubules (Figure 1D, Supplemental Figure 2).

Tsc1 Deletion in Renal Proximal Tubules Activated Aberrant mTORC1 Signaling

The mTORC1 phosphorylation target, 4E-BP1, migrates as at least 4–5 bands, denoted α, β, γ, δ, and ε (Figure 1F),

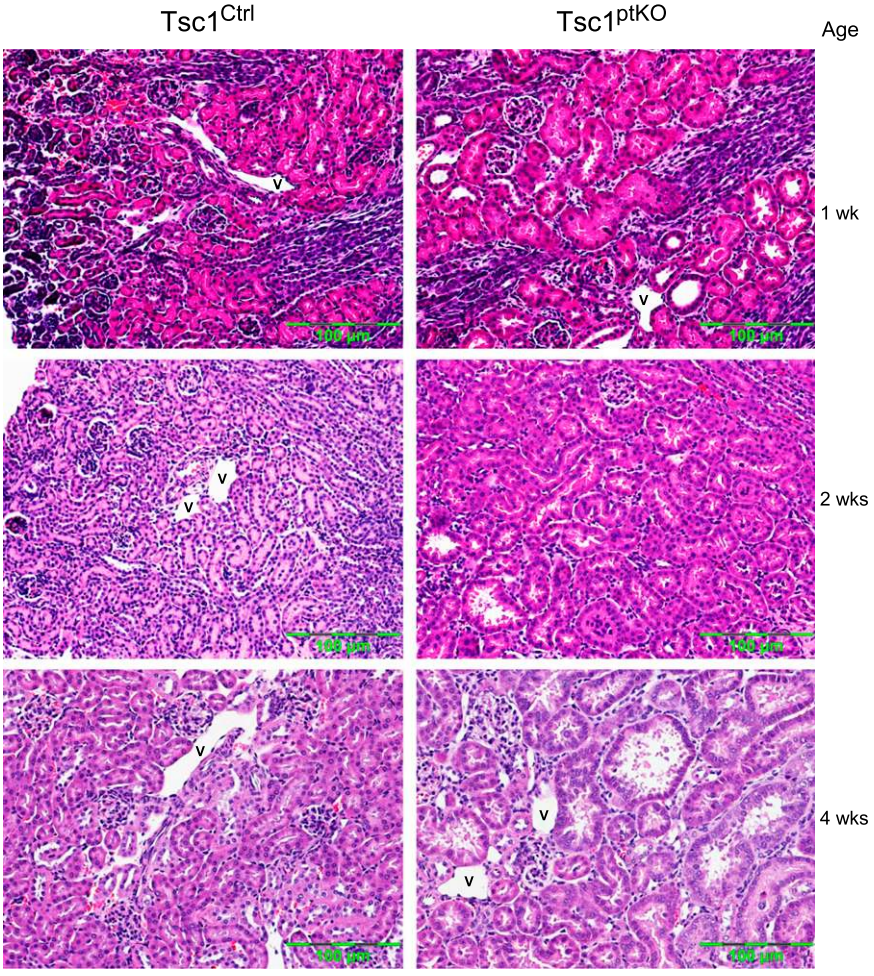

Figure 2. Deletion of Tsc1 in renal proximal tubular epithelial cells caused cellular hypertrophy and proliferation, consequently resulting in tubular hypertrophy. H&E-stained kidney sections revealed that renal proximal tubule cell-specific Tsc1 knockout (Tsc1^{ptKO}) mice had markedly enlarged renal proximal tubules lined with hyperplastic and hypertrophic epithelial cells, compared with their gender- and age-matched littermate control (Tsc1^{Ctrl}) mice at 1, 2, and 4 weeks of age. Shown are representative images from *n* of at least five animals/group with similar results. (Scale bar, 100 μm.)

representing 4E-BP1 phosphorylated to varying extents as previously reported.[14,32,33] The 4E-BP1 species with higher apparent relative molecular mass (ε- and δ-species), but not the lowest α-species, were aberrantly upregulated in Tsc1^{ptKO} kidneys, indicating that persistent mTORC1 activation induced by genetic *Tsc1* deletion ultimately led to an accumulation of the hyperphosphorylated species of 4E-BP1 (Figure 1F). This is consistent with the fact that the hyperphosphorylated species of 4E-BP1 are stable and refractory to degradation by the ubiquitin-proteasome pathway.[34] When separated well, band shift was also seen for the 2–3 species of rpS6, owing to its phosphorylation to different degrees at multiple serine residues.[30,35] Immunoblotting with phospho-specific antibodies confirmed that the phosphorylation levels of both 4E-BP1 and rpS6 were markedly increased in Tsc1^{ptKO} kidneys, thus confirming mTORC1 activation (Figure 1F). Immunohistochemistry localized the increased phospho-rpS6 (p-rpS6) and phospho-4E-BP1 (p-4E-BP1) to the activated proximal tubular epithelial cells in Tsc1^{ptKO} mice (Figure 1G). In contrast, Tsc1^{Ctrl} mice had very low basal levels of p-4E-BP1 and p-rpS6 in proximal tubules and moderate levels in distal nephron segments, in which a subset of cells express a relatively high basal level of p-rpS6 (Figure 1G). Cellular hypertrophy- and hyperplasia-caused proximal tubule enlargement was already striking enough by 1 week of age, as clearly shown in Figure 2.

Genetic Deletion of rpS6 Phosphorylation in Tsc1^{ptKO} Mice Transiently Inhibited Cell Proliferation and Kidney Growth but Subsequently Exacerbated Cystogenesis

A mutated *rpS6* allele was knocked into the locus of mouse *rpS6* gene to generate *rpS6* knockin mice expressing nonphosphorylatable rpS6 (rpS6$^{P-/-}$), in which all five phosphorylatable serine residues encoded by the exon 5 of *rpS6* were replaced with alanine residues, as depicted in Figure 3A.[30] By crossing these knockin mice with our new Tsc1^{ptKO} mouse line, we generated *Tsc1* and *rpS6* double gene-deficient mice, which express nonphosphorylatable rpS6 throughout the whole body but their *Tsc1* gene was knocked out only in renal proximal tubules (Tsc1^{ptKO};rpS6$^{P-/-}$), as depicted in Figure 3B. Immunoblotting confirmed complete deletion of S235/236-phosphorylated rpS6 (Figure 3C) and S240/244-phosphorylated rpS6 (data not shown) in Tsc1^{ptKO};rpS6$^{P-/-}$ mice and Tsc1^{Ctrl};rpS6$^{P-/-}$ mice while Tsc1^{ptKO} mice had markedly increased rpS6 phosphorylation, compared with Tsc1^{Ctrl} mice (Figure 3C).

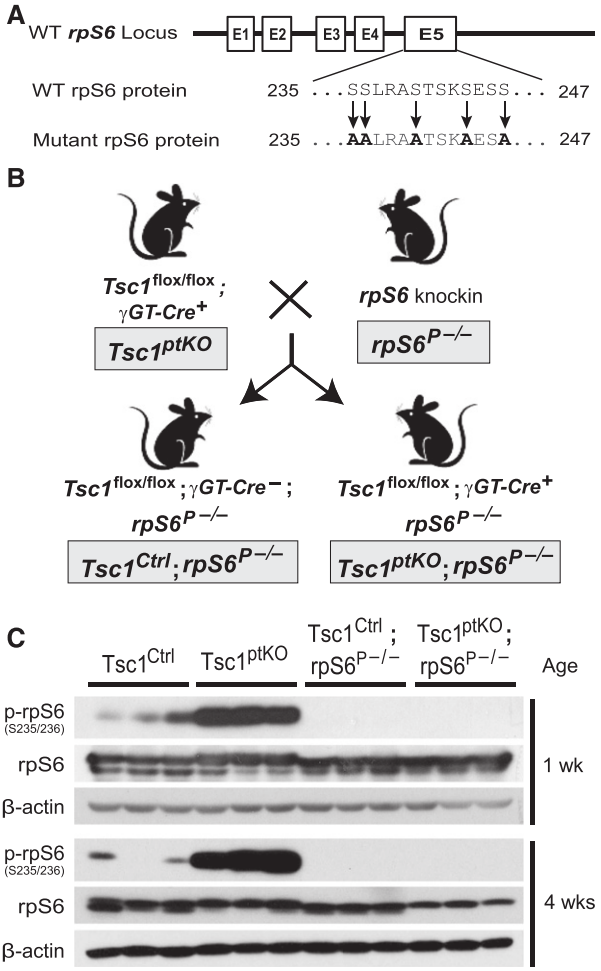

Figure 3. Generation of *Tsc1* and *rpS6* double gene-deficient mice. (A) Strategy for making rpS6$^{P-/-}$ knockin mice expressing nonphosphorylatable ribosomal protein rpS6, in which all five phosphorylatable serines (S235, S236, S240, S244, and S247) were replaced with alanines by site-directed mutagenesis. (B) A schematic depicting genetic deletion of rpS6 phosphorylation in the whole animal on the background of renal proximal tubule–specific *Tsc1* knockout (Tsc1^{ptKO}) mice, resulting in *Tsc1* and *rpS6* double gene–deficient (*Tsc1^{ptKO};rpS6$^{P-/-}$*) mice and *Tsc1^{Ctrl};rpS6$^{P-/-}$* littermates, used as control for genetic rpS6 phosphorylation deletion alone. (C) Immunoblotting of renal cortices confirmed complete deletion of rpS6 phosphorylation in *rpS6$^{P-/-}$* knock-in mice (*Tsc1^{Ctrl};rpS6$^{P-/-}$*) as well as the double gene–deficient *Tsc1^{ptKO};rpS6$^{P-/-}$* mice by 1 and 4 weeks of age. Shown are representative blots from at least three separate experiments with similar results.

Within 1 week of age, Tsc1 knockout-induced kidney growth was completely prevented in Tsc1^{ptKO};rpS6$^{P-/-}$ mice, as indicated by normalized kidney to body weight ratios (Figure 4A), with indistinguishable body weights (Figure 4B) and similar proliferating cell numbers outside of proximal tubules (Figure 5A) but a significantly inhibited proliferating cell number in the proximal tubules (Figure 5B), compared with Tsc1^{ptKO} mice. Surprisingly, by 2 weeks of age, Tsc1^{ptKO};rpS6$^{P-/-}$ mice had a significantly rebounded and sustained rate of cell proliferation in the proximal tubules (Figure 5, A and B) and their kidneys outgrew those of Tsc1^{ptKO} mice (Figure 4A), with more pronounced renal cysts (Figure 4D). By 4 weeks of age, Tsc1^{ptKO};rpS6$^{P-/-}$ mice developed much more severe cystic kidneys (Figure 4D, Supplemental Figure 3) and tubulointerstitial fibrosis revealed by Masson's trichrome staining (Figure 6A) and immunohistochemical staining for fibronectin (Figure 6B), with occasional glomerular cysts in the most severe cystic areas (Supplemental Figure 4). These pathologic

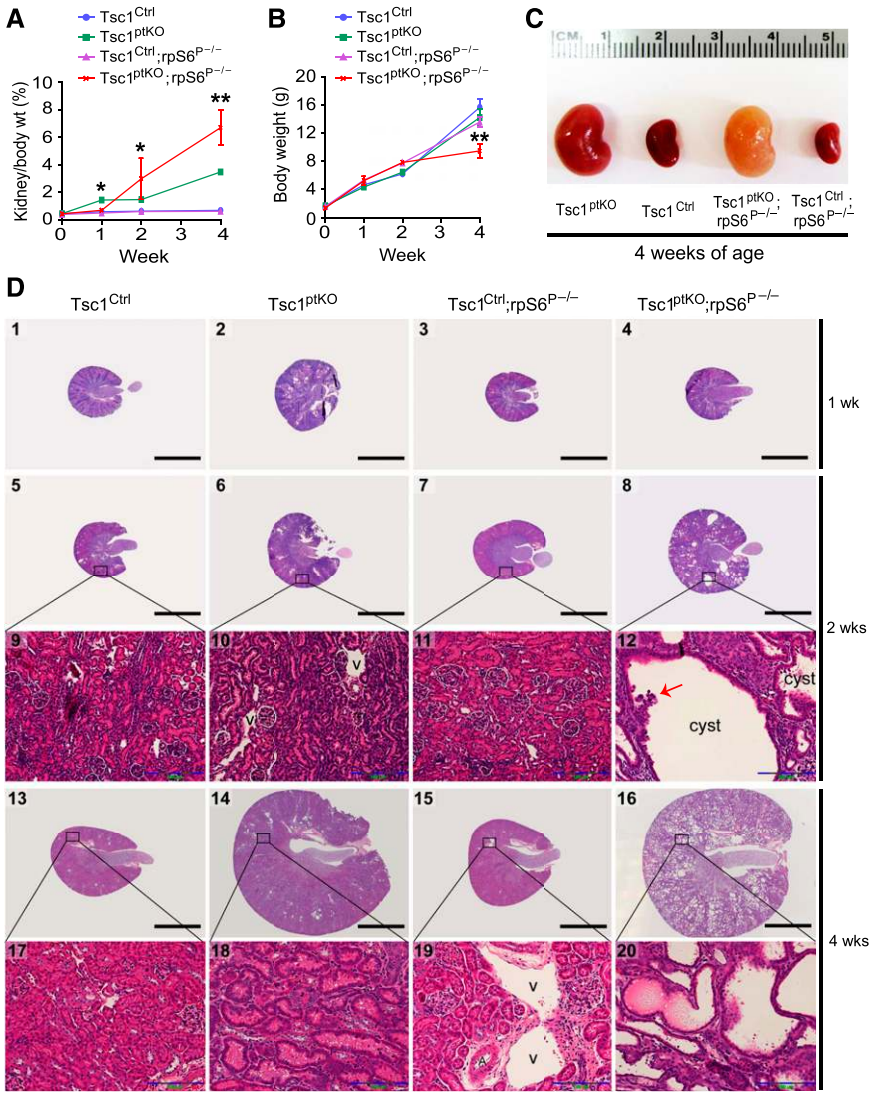

Figure 4. Genetic deletion of rpS6 phosphorylation transiently prevented *Tsc1* deletion-induced kidney growth within 1 week of age but subsequently exacerbated cystogenesis in *Tsc1*-deleted kidneys. (A) Kidney to body weight ratios and (B) body weights of all four genotypes of mice at the indicated age. Data are expressed as means±SEM; *$P<0.05$, **$P<0.01$ for Tsc1^{ptKO} mice versus *Tsc1^{ptKO};rpS6$^{P-/-}$* mice at 1, 2, and 4 weeks of age, respectively. (C) Representative kidney images of indicated four genotypes of mice at 4 weeks of age. (D) H&E staining demonstrated transient inhibition of kidney growth and cystogenesis in *Tsc1^{ptKO};rpS6$^{P-/-}$* mice compared with Tsc1^{ptKO} mice within 1 week of age, but compared with Tsc1^{ptKO} mice, *Tsc1^{ptKO};rpS6$^{P-/-}$* mice developed worsening cystogenesis after 1 week of age. In contrast, both *Tsc1^{Ctrl};rpS6$^{P-/-}$* mice as well as Tsc1^{Ctrl} mice exhibited normal kidney histology. (Scale bars: 2 mm in all images of *D1–8* and *D13–16*; 100 μm in all images of *D9–12* and *D17–20*). $n\geq5$ mice per genotype group at each time point. A in D19 indicates an artery; V in *D10* and *D19* indicates veins; the red arrow in *D12* indicates papillary tumorous growth inside a renal cyst.

changes caused a pale appearance of the enlarged kidneys (Figure 4C) and a retardation of the animal growth, as shown by significantly lower body weights (Figure 4B) and consequently much higher kidney to body weight ratios (Figure 4A). Tsc1^{ptKO} mice developed enormous kidneys (Figure 4C) due to cellular hypertrophy– and hyperplasia–caused enlargement of proximal tubules (Figures 1D and 2), with only a few focal microscopic renal cysts (Figure 4D, Supplemental Figure 5). There was no cystic kidney lesion in Tsc1^{Ctrl};rpS6$^{P-/-}$ mice (Figure 4D). Tsc1^{ptKO};rpS6$^{P-/-}$ mice developed significantly increased BUN by 2 weeks of age, indicating impaired renal function (Figure 6C), with 67% premature death by 9 weeks of age when Tsc1^{ptKO} mice were all alive (Figure 6D).

Immunofluorescence staining with the proximal tubule marker, *Lotus-tetragonolobus Lectin* (LTL), and the distal tubule/collecting duct marker, *Dolichos biflorus Agglutinin* (DBA), confirmed that all renal cysts originated from proximal tubules (Figure 7A). Some epithelial cells lining the larger cysts seen in Tsc1^{ptKO} mice, and especially in Tsc1^{ptKO};rpS6$^{P-/-}$ mice, by 4 weeks of age did not show cross-reactivity to LTL (Figure 7B), suggesting that these cells have lost their differentiated characteristics as the cysts enlarge further; consistent with this de-differentiation was that virtually all the Ki67-positive (proliferating) cells lining these larger cysts were negative for LTL, although not all LTL-negative cyst-lining cells were captured for Ki67 positivity (Figure 7B).

Genetic Deletion of rpS6 Phosphorylation in Tsc1^{ptKO} Mice Transiently Inhibited Phosphorylation of both S6K1 and 4E-BP1, with Subsequent Accumulation of Hyperphosphorylated 4E-BP1

By 4 weeks of age, the phosphorylation of both S6K1 and 4E-BP1 in Tsc1^{ptKO} mice markedly declined compared with that of 1-week-old Tsc1^{ptKO} mice, but was still elevated compared with that of Tsc1^{Ctrl} mice (Figure 8, A and B). Genetic deletion of rpS6 phosphorylation in Tsc1^{ptKO} mice inhibited both S6K1 and 4E-BP1 phosphorylation within 1 week of age (Figure 8A), but such an inhibition was lost subsequently, with a marked accumulation of hyperphosphorylated species of 4E-BP1, as evidenced by nearly all 4E-BP1 bands being shifted to the top band and confirmed by increased S65-hyperphosphorylated 4E-BP1 in Tsc1^{ptKO};rpS6$^{P-/-}$ mice by 4 weeks of age (Figure 8B). Immunohistochemistry localized the hyperphosphorylated 4E-BP1 to the epithelial cells lining the enlarged/dilated renal tubules and renal cysts (Figure 8C) and also localized to the cells forming microscopic renal tumors (Supplemental Figure 7).

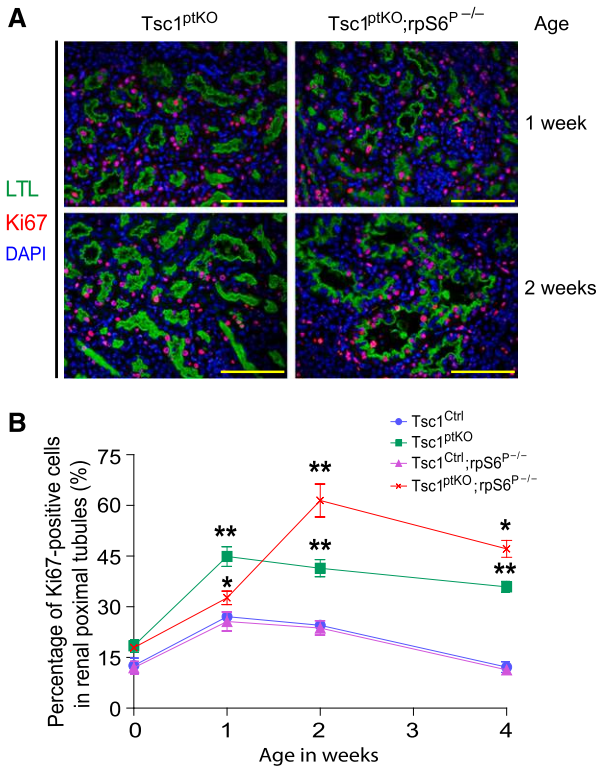

Figure 5. Genetic deletion of rpS6 phosphorylation on the background of Tsc1^{ptKO} mice transiently inhibited but subsequently stimulated cell proliferation in renal proximal tubules. (A,B) Triple immunofluorescence staining with LTL to label renal proximal tubules, a Ki67 antibody to label proliferating cells and DAPI to label nuclei detected similarly abundant proliferating cells outside of proximal tubules in both Tsc1^{ptKO} and *Tsc1^{ptKO};rpS6$^{P-/-}$* mice at 1–2 weeks of age (A); however, Tsc1^{ptKO} mice exhibited significantly increased Ki67-positive cells in the proximal tubules compared with other groups of mice at and after 1 week of age, but *Tsc1^{ptKO};rpS6$^{P-/-}$* mice had a higher percentage of Ki67-positive cells in the proximal tubules than that in Tsc1^{ptKO} mice by 2 weeks of age and remained elevated even by 4 weeks of age (B). The percentage of Ki67-positive cells was calculated from 25 randomly captured images for each group (five images per mouse, five mice per group) at each time point at the original magnification of 400× from the LTL-positive region. Only Ki67-positive nuclei within LTL-positive tubules were counted for the numerator, which was divided by the sum of Ki67-positive nuclei and DAPI-positive nuclei within the LTL-positive tubules and then multiplied by 100%. Data are expressed as means±SEM, *P<0.05 for Tsc1^{ptKO} versus *Tsc1^{ptKO};rpS6$^{P-/-}$* at both 1 week and 4 weeks of age. **P<0.001 for *Tsc1^{ptKO};rpS6$^{P-/-}$* versus Tsc1^{ptKO} mice at 2 weeks of age as well as Tsc1^{ptKO} versus Tsc1^{Ctrl} and *Tsc1^{Ctrl};rpS6$^{P-/-}$* mice at 1, 2, and 4 weeks of age, respectively.

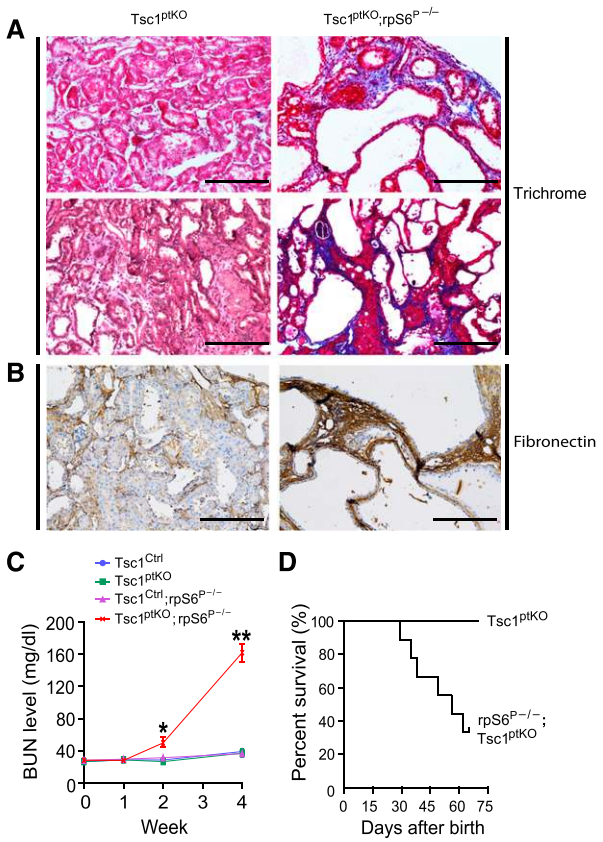

Figure 6. Genetic deletion of rpS6 phosphorylation on the background of Tsc1^{ptKO} mice exacerbated interstitial fibrosis, impaired kidney function, and caused premature animal death. (A) Masson's trichrome staining and (B) immunohistochemical staining for fibronectin revealed markedly more severe interstitial fibrosis in *Tsc1^{ptKO};rpS6$^{P-/-}$* mice than in Tsc1^{ptKO} by 4 weeks of age. Shown are representative images from n of five mice per genotype with similar results. (Scale bars, 200 μm.) (C) Statistically significant increases in BUN in Tsc1^{ptKO};rpS6$^{P-/-}$ mice indicated a decline of renal function. Data are expressed as means±SEM *P<0.05, **P<0.01 for *Tsc1^{ptKO};rpS6$^{P-/-}$* compared with other three genotypes of mice at 2 and 4 weeks of age, respectively; n=5 mice/group. (D) *Tsc1^{ptKO};rpS6$^{P-/-}$* mice displayed an increased mortality after 4 weeks of age (n=7 for Tsc1^{ptKO} mice, n=9 for *Tsc1^{ptKO};rpS6$^{P-/-}$* mice).

Rapamycin Inhibited Tsc1 Deletion-Induced mTORC1 Activation and Kidney Growth but Exacerbated Cystic Kidney Lesions

Treating Tsc1^{ptKO} mice with the mTORC1 inhibitor rapamycin markedly inhibited S6K1 and rpS6 phosphorylation; it also suppressed hyperphosphorylation and accumulation of total 4E-BP1 (Figure 9A). This dramatically reduced Tsc1 deletion-induced kidney growth (Figure 9B), decreased kidney to body weight ratio (Figure 9C), increased the size of renal cysts (Figure 9B), elevated BUN levels (Figure 9D), and caused significant premature death within 2 weeks of treatment (Figure 9E). Renal histology confirmed that rapamycin markedly increased the size of renal cysts in the shrunken kidneys (Figure 10A) and exacerbated tubulointerstitial fibrosis as confirmed by Masson trichrome staining (Figure 10B) and immunohistochemistry for fibronectin (Figure 10C). Higher magnification light microscopy revealed that vehicle-treated Tsc1^{ptKO} mice consistently showed enlarged renal tubules and focal microscopic cysts lined with multilayers of proliferating cells and microscopic renal tumors consisting of aberrantly

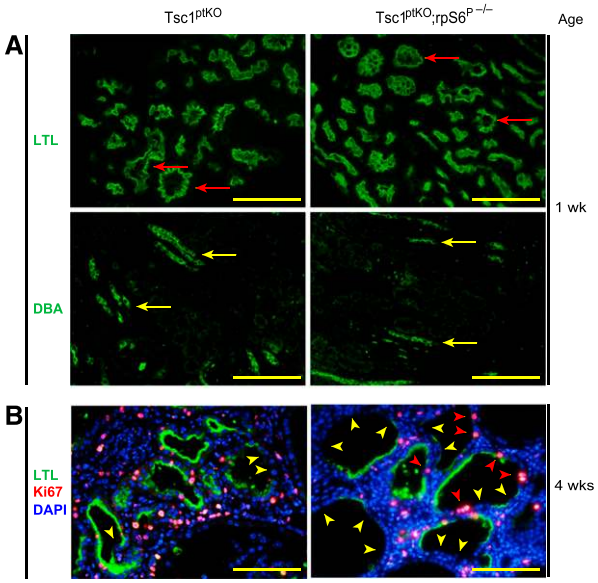

Figure 7. Kidney cysts in both Tsc1^{ptKO} and *Tsc1^{ptKO};rpS6$^{P-/-}$* mice originated from proximal tubules. (A) Immunofluorescence staining with the proximal tubule marker LTL (green) or the distal tubule/collecting duct marker DBA (green), respectively confirmed that all renal cysts originated from proximal tubules (red arrows), but not from DBA-positive tubules (yellow arrows). (B) Triple immunofluorescence staining with LTL (green), DAPI (blue, labeling nuclei), and an antibody against Ki-67 (red, labeling proliferating cells) revealed loss of LTL staining (yellow arrowheads), indicative of dedifferentiation, in some but not all epithelial cells, particularly those lining the larger cysts in *Tsc1^{ptKO};rpS6$^{P-/-}$* mice, by 4 weeks of age, with virtually all Ki67-positive cyst-lining cells being negative for LTL. (Scale bar, 100 μm.)

proliferating cells (Figure 11A, top panels), similar to those seen in untreated Tsc1^{ptKO} mice (Figure 1D). Notably, rapamycin treatment caused sloughing off and death of the multilayers of proliferating cells lining the enlarged renal tubules (thus seemingly enlarging cyst size) and also caused death of the cells forming the center of the microscopic renal tumors and resulted in a lesion appearing as central liquefaction necrosis (thus seemingly "turning" the tumors into cysts), as indicated in the lower panels of Figure 11, A and B.

DISCUSSION

In *Drosophila*, both dS6K and d4E-BP regulate cell growth (increase in cell size) and cell proliferation (increase in cell number).[36,37] In mammals, different mechanisms might have been evolved to regulate cell growth and proliferation separately.[38,39] It has been demonstrated that 4E-BPs mediate mTORC1 effects to promote cell proliferation, but not growth, in mammalian cells.[40] Here we provide evidence that both cellular hypertrophy and hyperplasia contribute to the enlargement of renal proximal tubules, with a few small cysts and occasional microscopic tumors, consequently resulting in strikingly enlarged kidneys in Tsc1^{ptKO} mice. These findings unveil an essential role for Tsc1 in controlling the normal size and homeostasis of the kidneys. Mechanistic studies confirmed markedly activated mTORC1, supporting our hypothesis that mTORC1 is a "common denominator" mediating kidney growth.

Phosphorylation of rpS6 is implicated in the regulation of cell growth and proliferation in multiple cell types.[7,20,25,29,30] Surprisingly, genetically blocking rpS6 phosphorylation in Tsc1^{ptKO} mice only transiently inhibited cell proliferation and kidney growth as the kidneys of rpS6$^{P-/-}$;Tsc1^{ptKO} mice soon developed aberrantly rebounded cell proliferation and outgrew the kidneys of Tsc1^{ptKO} mice, causing exacerbated cystogenesis and fibrosis. This might suggest a previously unappreciated role of rpS6 phosphorylation in suppressing renal cystogenesis and fibrosis. Genetically blocking rpS6 phosphorylation in Tsc1^{ptKO} mice only transiently inhibited mTORC1 signaling, through an unknown mechanism, possibly suggesting the existence of a previously unrecognized positive-feedback loop exerted by S6K1-mediated rpS6 phosphorylation on mTORC1 activity. Thus, deleting such a regulatory loop reduced mTORC1 signaling to phosphorylation of both S6K1 and 4E-BP1. This hypothesis certainly deserves further investigation in future studies to delineate the detailed molecular signaling steps.

Unlike 4E-BP1, no accumulation or upregulation of total S6K1 and total rpS6 was observed in any of the four genotypes of mice used in the current study, although we could not completely rule out whether nonphosphorylatable rpS6 could have a nonphysiologically relevant dominant negative effect in the setting of Tsc1 deletion-induced mTORC1 activation. Furthermore, studying Tsc1^{Ctrl};rpS6$^{P-/-}$ mice confirmed that deletion of rpS6 phosphorylation in the quiescent kidneys of WT control mice (Tsc1^{Ctrl}) neither upregulated total 4E-BP1 nor altered mTORC1 signaling. Tsc1^{Ctrl};rpS6$^{P-/-}$ mice did not develop renal cysts or tumors, either. However, in the face of genetic *Tsc1* deletion–induced persistent mTORC1 activation, complete loss of the S6K1-phosphorylating sites in the mutant substrate rpS6 appeared to ultimately result in an accumulation of hyperphosphorylated 4E-BP1. Such signaling alterations might be the mechanism of aberrantly rebounded cell proliferation, consequently leading to increased cystogenesis and exacerbated fibrosis. This would be consistent with the demonstration that mTORC1-mediated cell proliferation, but not cell growth, is controlled by the 4E-BPs.[40] Of interest, 4E-BP1 is the most abundant isoform of the 4E-BPs in the majority of tissues (with some exceptions, such as brain).[41]

Pharmacologic treatment of Tsc1^{ptKO} mice with the mTORC1 inhibitor rapamycin nearly completely blocked mTORC1 signaling to phosphorylation of 4E-BP1, S6K1, and rpS6, consequently causing cell death, especially the aberrantly proliferating cells lining the renal tubules or forming the center of microscopic renal tumors, thus manifesting as enlarged cystic lesions and worsened renal fibrosis, consequently resulting in significantly impaired renal function

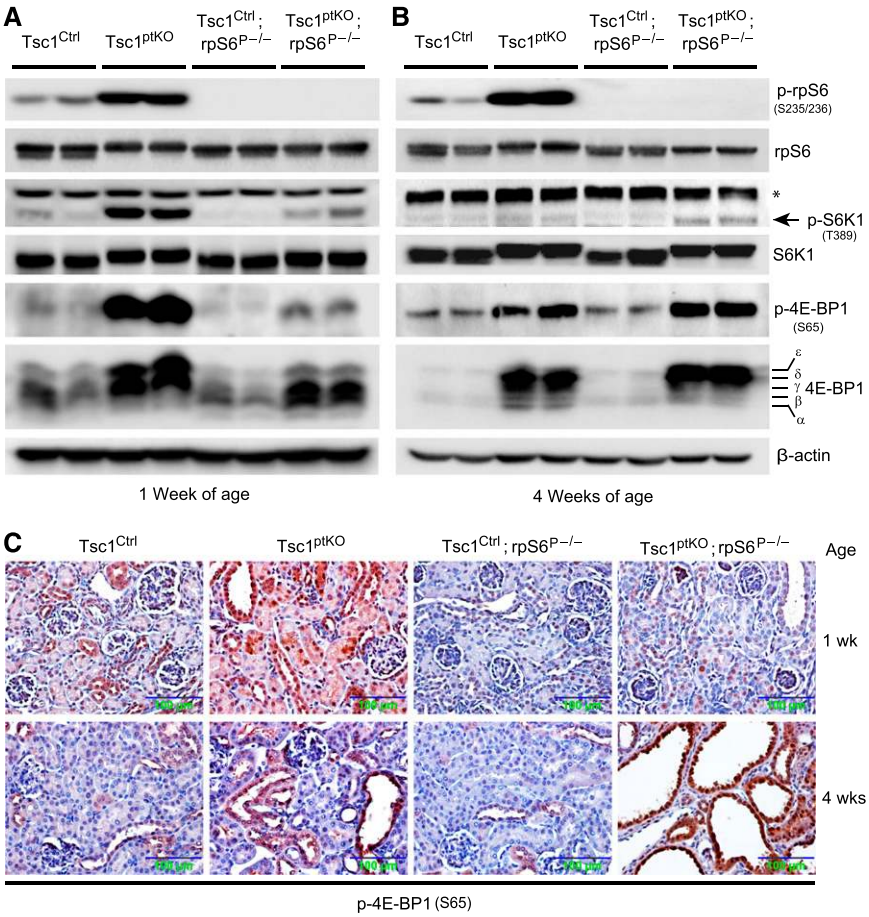

Figure 8. (A) Genetic deletion of rpS6 phosphorylation in $Tsc1^{ptKO}$ mice transiently inhibited Tsc1 knockout-activated mTORC1 signaling to phosphorylation of both S6K1 and 4E-BP1 within 1 week of age, (B) but subsequently accumulated the hyperphosphorylated species of 4E-BP1, as revealed by nearly all 4E-BP1 bands being shifted to the top band and further confirmed by increased S65-hyperphosphorylated 4E-BP1 species, consequently increasing the level of total 4E-BP1, in $Tsc1^{ptKO}$; $rpS6^{P-/-}$ mice by 4 weeks of age. *Denotes a nonspecific band. (C) Immunohistochemistry localized Tsc1 deletion-induced 4E-BP1 hyperphosphorylation to the epithelial cells lining the enlarged or dilated renal tubules and renal cysts. Shown are representative immunoblots and immunohistochemical staining images from at least five mice per genotype with similar results. (Scale bar: 100 μm.)

and premature animal death, despite markedly decreasing kidney size and destroying tumors. Thus, monitoring whole kidney volume alone for therapeutic efficacy could be misleading.

An intriguing question is: which is possibly the more detailed mechanism responsible for the markedly upregulated total 4E-BP1 in both $Tsc1^{ptKO}$ and $Tsc1^{ptKO}$;$rpS6^{P-/-}$ kidneys? In this regard, the abundance of the eukaryotic translation initiation factor 4E (eIF4E) is much lower than other translation factors and thus eIF4E is a rate-limiting factor in translation initiation.[42,43] Activation of mTORC1 mediates hyperphosphorylation of 4E-BP1,[12] consequently leading to its dissociation from eIF4E.[11] The released eIF4E binds to the 5′-cap structure of mRNAs and, together with eIF4G and eIF4A, assembles the translation initiation complex eIF4F, thus promoting the protein synthesis needed for cell proliferation.[11,12] With persistent mTORC1 activation (as in the kidneys of both $Tsc1^{ptKO}$ mice and $Tsc1^{ptKO}$;$rpS6^{P-/-}$ mice due to permanent deletion of the *Tsc1* gene), eIF4E is being actively engaged in the eIF4F complex, and thus is hardly available for binding to the scarce hypophosphorylated 4E-BP1. Further, recent studies have demonstrated that the hyperphosphorylated species of 4E-BP1 is stable and refractory to degradation (and thus tends to accumulate) while the eIF4E-unbound hypophosphorylated 4E-BP1 is unstable and readily degraded by the ubiquitin-proteasome pathway.[34] Hence, such a hyperphosphorylation-dependent molecular mechanism of 4E-BP1 stability might be responsible for the upregulation of 4E-BP1 abundance, particularly the hyperphosphorylated species of 4E-BP1 but not the hypophosphorylated α-species of 4E-BP1 seen in $Tsc1^{ptKO}$;$rpS6^{P-/-}$ mice by 4 weeks of age. Given the previously demonstrated role of 4E-BPs in mediating mTORC1-dependent cell proliferation,[40] it would be interesting to test whether selectively targeting 4E-BPs could block Tsc1 deletion–induced proliferative and cystic kidney lesions in future studies; 4E-BP1 knockout mice are viable and fertile with normal life span.[40,41]

Of patients with autosomal dominant polycystic kidney disease (ADPKD), around 85% are caused by mutations in the *PKD1* gene,[44] whereas most of the remaining 15% result from mutations in the *PKD2* gene.[45] However, typically the patients with ADPKD only develop a few renal cysts within the first two decades of life but numerous renal cysts can be found by the fifth decade. A "two-hit" hypothesis has been proposed to explain the focal and slow progressive feature of cyst formation and the significant heterogeneity of phenotypes within the same family with ADPKD. This "two-hit" model proposes that a germline mutation in one allele of a *PKD* gene as the first hit is not sufficient to cause cyst formation until a somatic mutation in another allele of the *PKD* gene has also occurred as the second hit later in life in a single cell, thus resulting in clonal proliferation of the cell into a cyst.[46–48] Germline homozygous deletion of *Pkd1* or *Pkd2* in mice causes perinatal lethality with numerous renal cysts.[49,50] Of interest, inactivation of *Pkd1* in adult mice causes a slow onset of cystic kidneys.[51–53] Inactivation of the ciliogenic gene *Kif3a* in adult mice did not cause rapid cyst formation despite the loss of primary cilia; however, ischemia-reperfusion

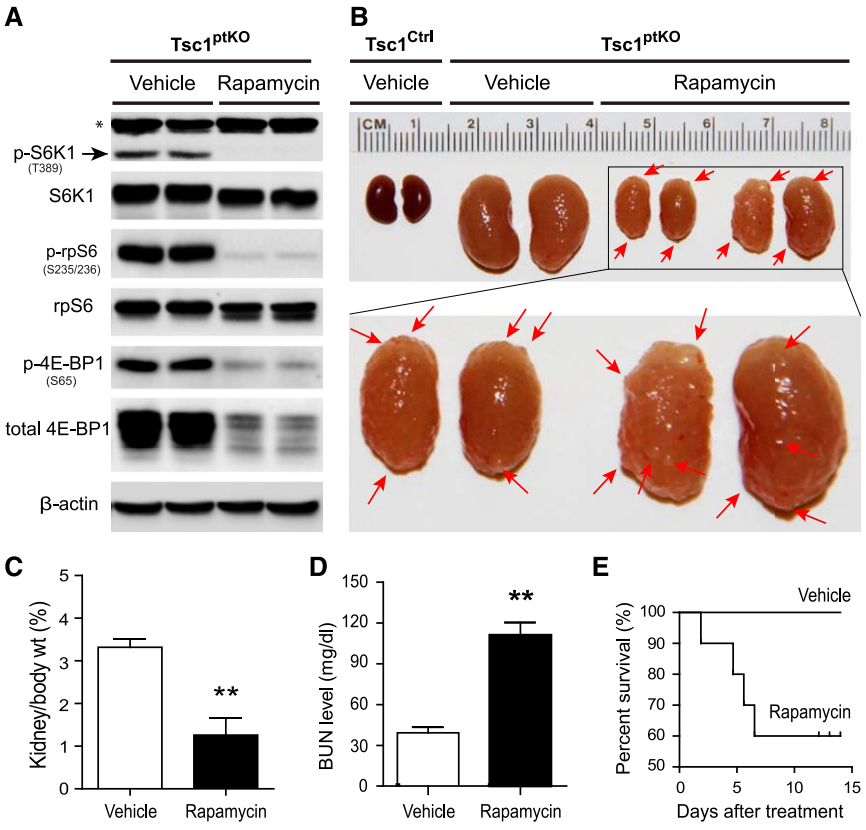

Figure 9. Rapamycin treatment inhibited mTORC1 signaling and kidney growth but caused renal failure and premature death in Tsc1^{ptKO} mice. (A) Rapamycin treatment (1 mg/kg body wt by intraperitoneal injection once every other day for 2 weeks starting from 2 weeks of age) inhibited S6K1, rpS6 and 4E-BP1 phosphorylation and decreased total 4E-BP1 levels in Tsc1^{ptKO} mice. *Denotes a nonspecific band. (B–E) Rapamycin inhibition of mTORC1 signaling in Tsc1^{ptKO} mice (B) decreased kidney size but increased cyst size, indicated by red arrows, (C) reduced kidney to body weight ratio, (D) increased BUN level, and (E) caused premature animal death. The representative immunoblots (A) and kidney images (B) are from *n* of 7–10 mice per group with similar results. Data in (C) and (D) are expressed as means±SEM; $^{**}P<0.01$ compared rapamycin-treated Tsc1^{ptKO} mice (n=10) to vehicle-treated Tsc1^{ptKO} mice (n=7).

renal (IRI) injury induced cyst formation in adult *Kif3a* mutant mice.[54] Thus, renal injury has been proposed to be a "third hit" that promotes rapid cyst formation in adult *Pkd1*-inactivated mouse kidneys.[55,56] Nephrotoxin-induced renal injury also significantly accelerated cyst formation in *Pkd1*-deleted mice.[57] IRI induces significant dilation of renal tubules and development of microcysts even in *Pkd1*-heterozygous mice but not in their WT control mice.[58] Moreover, uninephrectomy also accelerates renal cyst formation in adult mice without cilia due to conditional knockout of the primary cilia gene *ift88*.[16,59] This study observed that genetic elimination of rpS6 phosphorylation in conditional *Tsc1* knockout mice ultimately activated aberrant cell proliferation and promoted cyst formation. Therefore, it seems likely that after the homozygous deletion of a cyst-suppressing gene, including *Tsc1*, activated cell proliferation is a key common event that accelerates cyst formation and expansion. However, future studies are required to confirm whether deletion of rpS6 phosphorylation, IRI injury, nephrotoxins, or uninephrectomy could each act as a "third hit" to stimulate rapid cystogenesis after *Tsc1* or *Tsc2* deletion has been induced in adult mice. Apparently, cystogenesis is a much more complicated process than we initially thought because it involves alterations in many cellular and molecular signaling events,[60,61] not merely any single event, but our data support the notion that aberrantly activated cell proliferation is a major cellular mechanism that actively drives cystogenesis.

To date, there is no Food and Drug Administration-approved curative treatment for ADPKD to slow or stop cyst formation and cyst growth, although ADPKD remains the most common monogenic cause of kidney failure worldwide.[62,63] Of interest, the mTOR pathway is aberrantly activated in the cyst-lining epithelial cells in human patients with ADPKD[64] and in a mouse model of PKD induced by conditional inactivation of *Pkd1*,[65] the gene responsible for the majority of human patients with ADPKD. Further, mTOR inhibitors (rapamycin and everolimus) have been shown to increase apoptosis of cyst-lining cells, reduce cyst growth, inhibit renal fibrosis, decrease kidney size, and preserve renal function in both mouse and rat models of polycystic kidney disease (PKD).[64–71] In our present study, we also observed that rapamycin inhibition of the mTOR pathway markedly induced cell death and drastically reduced kidney size. However, in contrast to previous results, we surprisingly found that rapamycin increased the size of renal cysts, exacerbated renal fibrosis, and impaired renal function, as demonstrated in Figures 9–11. The reason(s) behind these conflicting findings is not immediately clear, even only compared with mouse PKD models. The major differences are that the conditional *Tsc1* knockout mice in our present study were generated by using the γGT promoter-driven Cre to delete the *Tsc1* gene in the proximal tubules (thus induced cellular hypertrophy and proliferation causing primarily proximal tubular hypertrophy, with some LTL-positive small renal cysts and microscopic hamartomatous renal tumors; no DBA-positive cysts were seen), whereas the conditional *Pkd1* knockout mice in the previous study were generated by using the Nestin promoter-driven Cre to delete the *Pkd1* gene and induced numerous renal cysts predominantly originated from collecting duct/distal tubules (no LTL-positive cysts were evident).[65] Furthermore, the genetic background

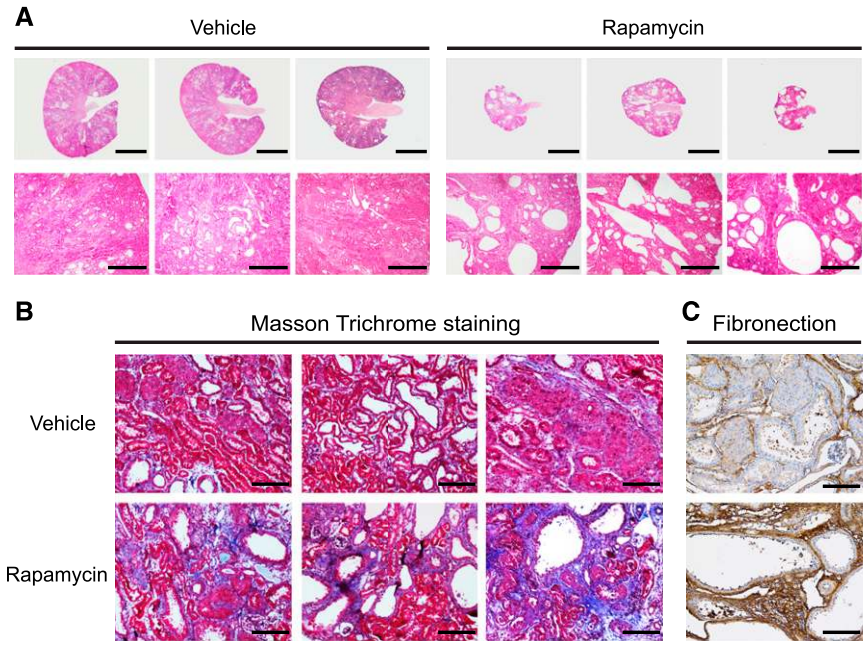

Figure 10. Rapamycin treatment of Tsc1^{ptKO} mice exacerbated cystic and fibrotic kidney lesions. (A,B) Renal histology confirmed that rapamycin treatment (as indicated in the legend of Figure 9A) (A) markedly increased cyst size, despite decreasing kidney size, and exacerbated tubulointerstitial fibrosis, which was confirmed by (B) trichrome staining and (C) increased fibronectin deposition revealed by immunohistochemistry. (Scale bars: 2 mm in upper panel of A; 500 μm in lower panel of A; and 200 μm in B and C.)

of our conditional *Tsc1* knockout mice is not identical to that of the conditional *Pkd1* knockout mice. Moreover, the conditional *Pkd1* knockout mice in the previous study were able to tolerate daily treatment with 5 mg/kg rapamycin (starting at 28 days of age and ending at 49 days of age); however, treatment of our conditional *Tsc1* knockout mice with 1 mg/kg once every other day for 2 weeks (starting from 2 weeks of age) already caused 40% premature death within 2 weeks.

Finally, it is noteworthy that although not all of the previous studies characterized the sensitivity of different nephron segment-derived cysts to rapamycin treatment, a more recent study by Shillingford *et al.* reported that after treatment with folate-conjugated rapamycin, which was demonstrated to be as effective as unconjugated rapamycin, only the DBA-positive (distal and collecting tubule) cysts diminished but the LTL-positive (proximal tubule) cysts increased in *bpk* mice, another commonly used mouse model of PKD that normally has a small percentage of proximal tubule cysts, as clearly demonstrated in their supplemental figure 3.[70] This observation is consistent with the inhibitory effect of rapamycin on cystogenesis in another mouse model that conditionally inactivated *Tsc1* in the distal convoluted tubules, but not in the proximal tubules, using *Emx1-Cre* mice, as reported by Armour *et al.*[71] and is also consistent with the worsening effect of rapamycin on cystogenesis in proximal tubule–specific Tsc1 knockout mice demonstrated in this study (Figures 9–11). Apparently, future studies are required to confirm and understand why proximal tubule–derived cysts are different from distal tubule- or collecting duct-derived cysts in their response to rapamycin treatment.

CONCISE METHODS

Reagents and Antibodies

Sheep anti-Tsc1 antibody and rabbit anti-sheep secondary antibody were purchased from R&D Systems (Minneapolis, MN). Antibodies against β-actin, phospho-S6K1 (p-S6K1), S6K1, p-rpS6, rpS6, p-4E-BP1, 4E-BP1, horse anti-mouse secondary antibody, and goat anti-rabbit secondary antibody were purchased from Cell Signaling Technology (Beverly, MA). Rabbit anti-Ki67, fluorescein-labeled LTL, fluorescein-labeled DBA, Dylight 549 anti-rabbit IgG, and Vectastain ABC Kit were purchased from Vector Labs (Burlingame, CA). Fibronectin antibody and other reagents were purchased from Sigma-Aldrich (St. Louis, MO).

Generation of Proximal Tubule-Specific *Tsc1* Gene Knockout Mice and *Tsc1-rpS6* Double Gene-Mutant Mice

Animals were housed at the Georgia Regents University veterinary facility (CA Building). Animal care and all experimental procedures were approved by Georgia Regents University's Institutional Animal Care and Usage Committee, and complied with the guidelines of National Institutes of Health. Renal proximal tubule cell-specific homozygous *Tsc1* gene knockout (Tsc1^{ptKO}) mice were generated by crossing *Tsc1$^{flox/flox}$* mice with a transgenic mouse line expressing Cre recombinase under the control of the gamma-glutamyl transpeptidase promoter (*γGT-Cre*).[31] The γGT-Cre mouse line has been used to successfully delete different genes of interest selectively in the renal proximal tubule.[31,72] *Tsc1$^{flox/flox}$* littermates lacking the *γGT-Cre* transgene (*Tsc1$^{flox/flox}$;γGT-Cre^{-}*) were used as control (Tsc1^{Ctrl}) mice, as depicted in Figure 1A.

To genetically delete phosphorylation of the ribosomal protein S6 (rpS6), an exon 5-mutant allele of the *rpS6* gene, in which the codons for all phosphorylatable serines were mutated to code for alanines (as depicted in Figure 4A), was knocked into the locus of WT *rpS6* gene by homologous recombination in 129Sv/J ES cells, as previously described.[30] The resultant homozygous *rpS6* knockin mice expressing nonphosphorylatable rpS6 (rpS6$^{P-/-}$) were further crossed with Tsc1^{ptKO} mice to generate Tsc1 and rpS6 double gene-mutant (*Tsc1^{ptKO};rpS6$^{P-/-}$*) mice, which were compared with the Tsc1 single knockout mice (Tsc1^{ptKO}), with gender-matched *Tsc1$^{flox/flox}$;γGT-Cre^{-};rpS6$^{P-/-}$* littermates (called Tsc1^{Ctrl};rpS6$^{P-/-}$ mice hereafter) as double control mice.

PCR Primers and Genotyping

Genomic DNA was isolated from mouse ear or tail biopsy samples for PCR genotyping. PCR primers used for the floxed-*Tsc1* allele

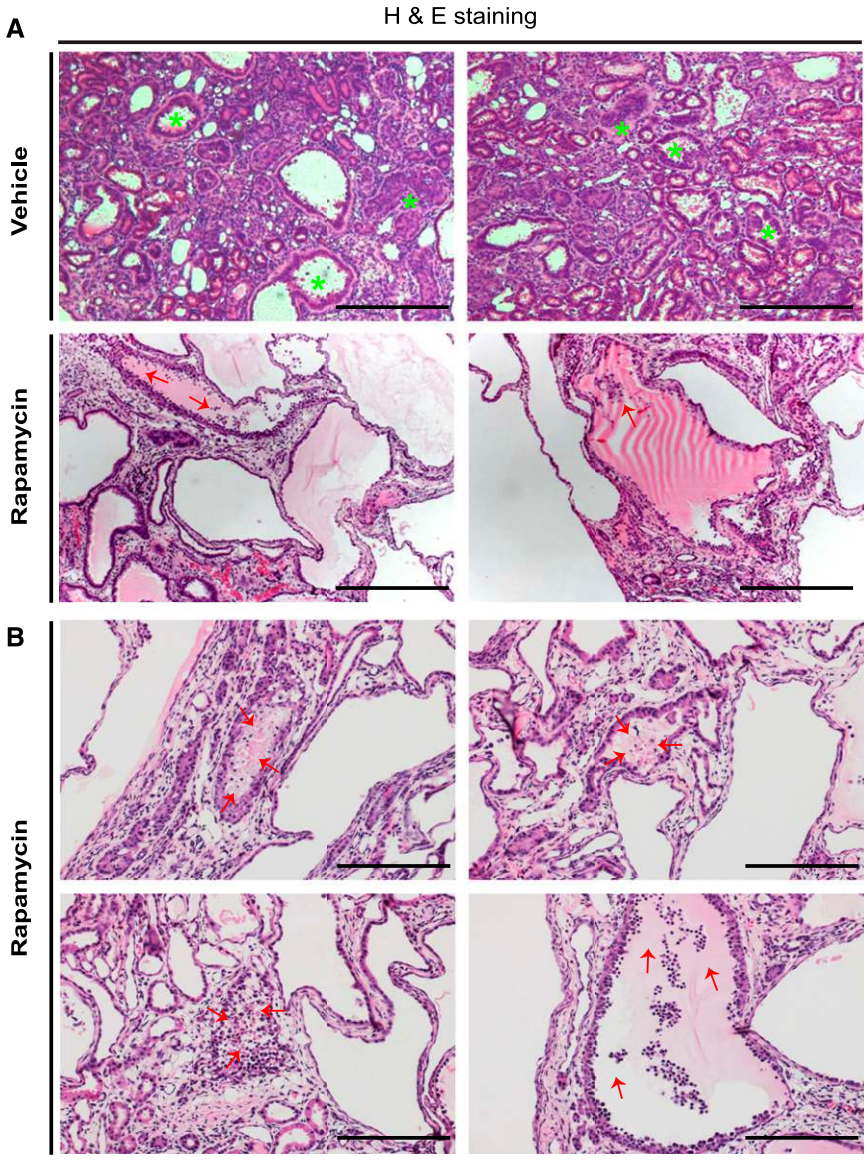

Figure 11. Rapamycin treatment caused death of proliferating epithelial cells in Tsc1^{ptKO} mice. (A,B) Tsc1^{ptKO} mice were treated with vehicle alone or rapamycin (1 mg/kg body wt) by intraperitoneal injection once every other day for 2 weeks starting from 2 weeks of age. Renal histology revealed that vehicle-treated Tsc1^{ptKO} mice consistently exhibited enlarged renal tubules and focal microscopic cysts lined with multilayers of proliferating cells and microscopic renal tumors consisting of aberrantly proliferating cells, marked by green asterisks (A, top panels), similar to those seen in untreated Tsc1^{ptKO} mice (Figure 1D). Rapamycin treatment caused sloughing off and death of the multilayers of proliferating cells lining the enlarged renal tubules (red arrows), thus seemingly enlarging cyst size (A, lower panels and B). Rapamycin also caused death of the cells forming the center of the microscopic renal tumors (red arrows) and destroyed the center of the tumors, causing a central liquefaction necrosis-like lesion in the microscopic renal tumors (seemingly "turning" the tumors into cysts, as indicated by red arrows (B). (Scale bars: 200 μm in A; 100 μm in B.)

are: 5′-GTCACGACCGTAGGAGAAGC-3′ and 5′-GAATCAACCCCACAGAGCAT-3′, while 5′-AGGTGTAGAGAAGGCACTTAGC-3′ and 5′-CTAATCGCCATCTTCCAGCAGG-3′ were used to detect the γGT-Cre transgene. PCR conditions for both floxed-*Tsc1* and γ*GT-Cre* are: 94°C for 1 min followed by 94°C for 10 s, 65°C for 30 s, and 72°C for 60 s for 30 cycles, with an additional 7-min extension at 72°C. For mutant *rpS6*, 5′-GTCATCCAGCATGGGTGCTG-3′ and 5′-GGCTGATACCTTTTGGGACAG-3′ were used as primers under the following PCR conditions: 95°C for 2 min followed by 94°C for 30 s, 52°C for 30 s, and 72°C for 60 s for 35 cycles, with a final extension at 72°C for 10 min, and the PCR products were digested by *Eco*R V at 37°C for 1 h to detect mutant rpS6.

Administration of Rapamycin to Tsc1^{ptKO} Mice and Examination of its Effects on the Kidneys

Rapamycin was purchased from LC Laboratories (Woburn, MA) and was administrated to Tsc1^{ptKO} mice at 1 mg/kg body wt by intraperitoneal injection every other day for 2 weeks (starting from 2 weeks of age). Fourteen days after rapamycin treatment when the survived mice were 4 weeks of age, the mice were sacrificed to harvest blood samples for measuring BUN, and kidneys were harvested for calculating kidney to body weight ratios and examining renal pathology by hematoxylin and eosin (H&E) staining, Masson's trichrome staining, immunohistochemistry staining for fibronectin and immunoblotting analysis for mTORC1 signaling to phosphorylation of S6K1, rpS6, and 4E-BP1, compared with Tsc1^{ptKO} mice treated with vehicle alone.

Histologic Examination, Immunohistochemistry, Immunofluorescence, and Immunoblotting Analysis

Mouse kidneys were fixed in 4% paraformaldehyde for paraffin-embedded kidney sections (5 μm), which were then deparaffinized and rehydrated for the following staining techniques. For histologic examination, H&E staining was performed using the standard methods.[73] Immunohistochemistry and immunofluorescence staining were performed as described previously.[73,74] Briefly, rehydrated kidney sections were subjected to antigen retrieval using the Antigen Unmasking Solution purchased from Vector, followed by blocking with 2% normal goat serum. The sections were then incubated with primary antibodies (indicated in the respective figures) at 4°C overnight, washed three times in PBS, incubated with appropriate secondary antibodies, and washed with PBS again. For immunohistochemistry, the signals were visualized using VECTASTAIN ABC kits (Vector), followed by counterstaining with hematoxylin and capturing images using a CX31

microscope with a DP73–1-51 digital camera (Olympus). For immunofluorescence staining, after incubation with the primary antibodies indicated and washing with PBS, the sections were incubated with Dylight 549-conjugated secondary antibodies and either DBA or LTL for 1 h, and images were captured using the OLYMPUS IX73 inverted 2-deck platform IX73 microscope system running on the CellSens Standard software. Immunoblotting analyses were performed as we previously described.[73–75]

Measurement of Kidney Function

BUN levels were measured as we previously described.[17,20] Briefly, blood samples were collected from mice at different ages indicated in the corresponding figures and BUN levels were immediately measured according to the instruction of the commercially available kit, Liquid Urea Nitrogen Reagent Set (Pointe Scientific).

Masson Trichrome Staining

Kidney sections (5 μm) were deparaffinized, rehydrated, and stained with the Trichrome Stain (Masson) Kit according to the manufacturer's instructions (Sigma-Aldrich, St. Louis, MO).

Statistical Analyses

Data are presented as means±SEM for at least three separate experiments (each in triplicate). An unpaired *t* test was used for statistical analysis, and ANOVA and Bonferroni *t* tests were used for multiple group comparisons using GraphPad Prism 6. A P value <0.05 compared with control was considered statistically significant.

ACKNOWLEDGMENTS

We are very grateful to Dr. Eric Neilson (Feinberg School of Medicine, Northwestern University) for providing the γGT-Cre mice. We also thank Dr. Thomas Weimbs (University of California Santa Barbara) for his helpful discussion.

This work was supported by funds from National Institutes of Health R01 Grant DK83575, and Start-up Funds from Georgia Regents University Augusta (to J.K.C.).

Some of the data in this paper were presented as an oral presentation during a free communication session at the 2013 American Society of Nephrology Annual Meeting, held November 5–10, 2013, in Atlanta, Georgia.

DISCLOSURES

None.

REFERENCES

1. Fine L: The biology of renal hypertrophy. *Kidney Int* 29: 619–634, 1986
2. Hostetter TH: Progression of renal disease and renal hypertrophy. *Annu Rev Physiol* 57: 263–278, 1995
3. Preisig PA: Renal hypertrophy and hyperplasia. In: *The Kidney*, edited by Selden DW, Giebisch G, 3rd Ed., Philadelphia, Lippincott Williams & Wilkins, 2000, pp 727–748
4. Brenner BM: Remission of renal disease: recounting the challenge, acquiring the goal. *J Clin Invest* 110: 1753–1758, 2002
5. Yoshida Y, Fogo A, Ichikawa I: Glomerular hemodynamic changes vs. hypertrophy in experimental glomerular sclerosis. *Kidney Int* 35: 654–660, 1989
6. Fogo A, Ichikawa I: Evidence for a pathogenic linkage between glomerular hypertrophy and sclerosis. *Am J Kidney Dis* 17: 666–669, 1991
7. Laplante M, Sabatini DM: mTOR signaling in growth control and disease. *Cell* 149: 274–293, 2012
8. Shimobayashi M, Hall MN: Making new contacts: the mTOR network in metabolism and signalling crosstalk. *Nat Rev Mol Cell Biol* 15: 155–162, 2014
9. Pearson RB, Dennis PB, Han JW, Williamson NA, Kozma SC, Wettenhall RE, Thomas G: The principal target of rapamycin-induced p70s6k inactivation is a novel phosphorylation site within a conserved hydrophobic domain. *EMBO J* 14: 5279–5287, 1995
10. Burnett PE, Barrow RK, Cohen NA, Snyder SH, Sabatini DM: RAFT1 phosphorylation of the translational regulators p70 S6 kinase and 4E-BP1. *Proc Natl Acad Sci U S A* 95: 1432–1437, 1998
11. Gingras AC, Raught B, Sonenberg N: eIF4 initiation factors: effectors of mRNA recruitment to ribosomes and regulators of translation. *Annu Rev Biochem* 68: 913–963, 1999
12. Gingras AC, Raught B, Sonenberg N: Regulation of translation initiation by FRAP/mTOR. *Genes Dev* 15: 807–826, 2001
13. Sarbassov DD, Ali SM, Kim DH, Guertin DA, Latek RR, Erdjument-Bromage H, Tempst P, Sabatini DM: Rictor, a novel binding partner of mTOR, defines a rapamycin-insensitive and raptor-independent pathway that regulates the cytoskeleton. *Curr Biol* 14: 1296–1302, 2004
14. Chen JK, Chen J, Neilson EG, Harris RC: Role of mammalian target of rapamycin signaling in compensatory renal hypertrophy. *J Am Soc Nephrol* 16: 1384–1391, 2005
15. Chen JK, Nagai K, Chen J, Plieth D, Hino M, Xu J, Sha F, Ikizler TA, Quarles CC, Threadgill DW, Neilson EG, Harris RC: Phosphatidylinositol 3-kinase signaling determines kidney size. *J Clin Invest* 125: 2429–2444, 2015
16. Bell PD, Fitzgibbon W, Sas K, Stenbit AE, Amria M, Houston A, Reichert R, Gilley S, Siegal GP, Bissler J, Bilgen M, Chou PC, Guay-Woodford L, Yoder B, Haycraft CJ, Siroky B: Loss of primary cilia upregulates renal hypertrophic signaling and promotes cystogenesis. *J Am Soc Nephrol* 22: 839–848, 2011
17. Chen JK, Chen J, Thomas G, Kozma SC, Harris RC: S6 kinase 1 knockout inhibits uninephrectomy- or diabetes-induced renal hypertrophy. *Am J Physiol Renal Physiol* 297: F585–F593, 2009
18. Sakaguchi M, Isono M, Isshiki K, Sugimoto T, Koya D, Kashiwagi A: Inhibition of mTOR signaling with rapamycin attenuates renal hypertrophy in the early diabetic mice. *Biochem Biophys Res Commun* 340: 296–301, 2006
19. Lee MJ, Feliers D, Mariappan MM, Sataranatarajan K, Mahimainathan L, Musi N, Foretz M, Viollet B, Weinberg JM, Choudhury GG, Kasinath BS: A role for AMP-activated protein kinase in diabetes-induced renal hypertrophy. *Am J Physiol Renal Physiol* 292: F617–F627, 2007
20. Xu J, Chen J, Dong Z, Meyuhas O, Chen JK: Phosphorylation of ribosomal protein S6 mediates compensatory renal hypertrophy. *Kidney Int* 87: 543–556, 2015
21. Norman JT, Fine LG: Renal growth and hypertrophy. In: *Textbook of Nephrology*, edited by Massry SG, Glassock RJ, Baltimore, Williams & Wilkins, 1995, pp 146–158.
22. Franch HA: Modification of the epidermal growth factor response by ammonia in renal cell hypertrophy. *J Am Soc Nephrol* 11: 1631–1638, 2000
23. van Slegtenhorst M, de Hoogt R, Hermans C, Nellist M, Janssen B, Verhoef S, Lindhout D, van den Ouweland A, Halley D, Young J, Burley M, Jeremiah S, Woodward K, Nahmias J, Fox M, Ekong R, Osborne J, Wolfe J, Povey S, Snell RG, Cheadle JP, Jones AC, Tachataki M, Ravine D, Sampson JR, Reeve MP, Richardson P, Wilmer F, Munro C, Hawkins TL, Sepp T, Ali JB, Ward S, Green AJ, Yates JR, Kwiatkowska J, Henske

EP, Short MP, Haines JH, Jozwiak S, Kwiatkowski DJ: Identification of the tuberous sclerosis gene TSC1 on chromosome 9q34. *Science* 277: 805–808, 1997
24. European Chromosome 16 Tuberous Sclerosis Consortium: Identification and characterization of the tuberous sclerosis gene on chromosome 16. *Cell* 75: 1305–1315, 1993
25. Meyuhas O, Dreazen A: Ribosomal protein S6 kinase from TOP mRNAs to cell size. *Prog Mol Biol Transl Sci* 90: 109–153, 2009
26. Yoon SO, Roux PP: Rapamycin resistance: mTORC1 substrates hold some of the answers. *Curr Biol* 23: R880–R883, 2013
27. Zaza G, Tomei P, Ria P, Granata S, Boschiero L, Lupo A: Systemic and nonrenal adverse effects occurring in renal transplant patients treated with mTOR inhibitors. *Clin Dev Immunol* 2013: 403280, 2013
28. Ruvinsky I, Katz M, Dreazen A, Gielchinsky Y, Saada A, Freedman N, Mishani E, Zimmerman G, Kasir J, Meyuhas O: Mice deficient in ribosomal protein S6 phosphorylation suffer from muscle weakness that reflects a growth defect and energy deficit. *PLoS One* 4: e5618, 2009
29. Volarevic S, Stewart MJ, Ledermann B, Zilberman F, Terracciano L, Montini E, Grompe M, Kozma SC, Thomas G: Proliferation, but not growth, blocked by conditional deletion of 40S ribosomal protein S6. *Science* 288: 2045–2047, 2000
30. Ruvinsky I, Sharon N, Lerer T, Cohen H, Stolovich-Rain M, Nir T, Dor Y, Zisman P, Meyuhas O: Ribosomal protein S6 phosphorylation is a determinant of cell size and glucose homeostasis. *Genes Dev* 19: 2199–2211, 2005
31. Iwano M, Plieth D, Danoff TM, Xue C, Okada H, Neilson EG: Evidence that fibroblasts derive from epithelium during tissue fibrosis. *J Clin Invest* 110: 341–350, 2002
32. Brunn GJ, Hudson CC, Sekulić A, Williams JM, Hosoi H, Houghton PJ, Lawrence JC Jr, Abraham RT: Phosphorylation of the translational repressor PHAS-I by the mammalian target of rapamycin. *Science* 277: 99–101, 1997
33. Hu C, Pang S, Kong X, Velleca M, Lawrence JC Jr: Molecular cloning and tissue distribution of PHAS-I, an intracellular target for insulin and growth factors. *Proc Natl Acad Sci U S A* 91: 3730–3734, 1994
34. Yanagiya A, Suyama E, Adachi H, Svitkin YV, Aza-Blanc P, Imataka H, Mikami S, Martineau Y, Ronai ZA, Sonenberg N: Translational homeostasis via the mRNA cap-binding protein, eIF4E. *Mol Cell* 46: 847–858, 2012
35. Krieg J, Hofsteenge J, Thomas G: Identification of the 40 S ribosomal protein S6 phosphorylation sites induced by cycloheximide. *J Biol Chem* 263: 11473–11477, 1988
36. Montagne J, Stewart MJ, Stocker H, Hafen E, Kozma SC, Thomas G: Drosophila S6 kinase: a regulator of cell size. *Science* 285: 2126–2129, 1999
37. Miron M, Verdú J, Lachance PE, Birnbaum MJ, Lasko PF, Sonenberg N: The translational inhibitor 4E-BP is an effector of PI(3)K/Akt signalling and cell growth in Drosophila. *Nat Cell Biol* 3: 596–601, 2001
38. Conlon I, Raff M: Differences in the way a mammalian cell and yeast cells coordinate cell growth and cell-cycle progression. *J Biol* 2: 7.1–7.10, 2003
39. Ohanna M, Sobering AK, Lapointe T, Lorenzo L, Praud C, Petroulakis E, Sonenberg N, Kelly PA, Sotiropoulos A, Pende M: Atrophy of S6K1(-/-) skeletal muscle cells reveals distinct mTOR effectors for cell cycle and size control. *Nat Cell Biol* 7: 286–294, 2005
40. Dowling RJ, Topisirovic I, Alain T, Bidinosti M, Fonseca BD, Petroulakis E, Wang X, Larsson O, Selvaraj A, Liu Y, Kozma SC, Thomas G, Sonenberg N: mTORC1-mediated cell proliferation, but not cell growth, controlled by the 4E-BPs. *Science* 328: 1172–1176, 2010
41. Tsukiyama-Kohara K, Poulin F, Kohara M, DeMaria CT, Cheng A, Wu Z, Gingras AC, Katsume A, Elchebly M, Spiegelman BM, Harper ME, Tremblay ML, Sonenberg N: Adipose tissue reduction in mice lacking the translational inhibitor 4E-BP1. *Nat Med* 7: 1128–1132, 2001
42. Hiremath LS, Webb NR, Rhoads RE: Immunological detection of the messenger RNA cap-binding protein. *J Biol Chem* 260: 7843–7849, 1985
43. Duncan R, Milburn SC, Hershey JW: Regulated phosphorylation and low abundance of HeLa cell initiation factor eIF-4F suggest a role in translational control. Heat shock effects on eIF-4F. *J Biol Chem* 262: 380–388, 1987
44. Consortium TEPKD; The European Polycystic Kidney Disease Consortium: The polycystic kidney disease 1 gene encodes a 14 kb transcript and lies within a duplicated region on chromosome 16. *Cell* 77: 881–894, 1994
45. Mochizuki T, Wu G, Hayashi T, Xenophontos SL, Veldhuisen B, Saris JJ, Reynolds DM, Cai Y, Gabow PA, Pierides A, Kimberling WJ, Breuning MH, Deltas CC, Peters DJ, Somlo S: PKD2, a gene for polycystic kidney disease that encodes an integral membrane protein. *Science* 272: 1339–1342, 1996
46. Reeders ST: Multilocus polycystic disease. *Nat Genet* 1: 235–237, 1992
47. Qian F, Watnick TJ, Onuchic LF, Germino GG: The molecular basis of focal cyst formation in human autosomal dominant polycystic kidney disease type I. *Cell* 87: 979–987, 1996
48. Wu G, D'Agati V, Cai Y, Markowitz G, Park JH, Reynolds DM, Maeda Y, Le TC, Hou H Jr, Kucherlapati R, Edelmann W, Somlo S: Somatic inactivation of Pkd2 results in polycystic kidney disease. *Cell* 93: 177–188, 1998
49. Lu W, Peissel B, Babakhanlou H, Pavlova A, Geng L, Fan X, Larson C, Brent G, Zhou J: Perinatal lethality with kidney and pancreas defects in mice with a targetted Pkd1 mutation. *Nat Genet* 17: 179–181, 1997
50. Wu G, Markowitz GS, Li L, D'Agati VD, Factor SM, Geng L, Tibara S, Tuchman J, Cai Y, Park JH, van Adelsberg J, Hou H Jr, Kucherlapati R, Edelmann W, Somlo S: Cardiac defects and renal failure in mice with targeted mutations in Pkd2. *Nat Genet* 24: 75–78, 2000
51. Piontek K, Menezes LF, Garcia-Gonzalez MA, Huso DL, Germino GG: A critical developmental switch defines the kinetics of kidney cyst formation after loss of Pkd1. *Nat Med* 13: 1490–1495, 2007
52. Lantinga-van Leeuwen IS, Leonhard WN, van der Wal A, Breuning MH, de Heer E, Peters DJ: Kidney-specific inactivation of the Pkd1 gene induces rapid cyst formation in developing kidneys and a slow onset of disease in adult mice. *Hum Mol Genet* 16: 3188–3196, 2007
53. Takakura A, Contrino L, Beck AW, Zhou J: Pkd1 inactivation induced in adulthood produces focal cystic disease. *J Am Soc Nephrol* 19: 2351–2363, 2008
54. Patel V, Li L, Cobo-Stark P, Shao X, Somlo S, Lin F, Igarashi P: Acute kidney injury and aberrant planar cell polarity induce cyst formation in mice lacking renal cilia. *Hum Mol Genet* 17: 1578–1590, 2008
55. Takakura A, Contrino L, Zhou X, Bonventre JV, Sun Y, Humphreys BD, Zhou J: Renal injury is a third hit promoting rapid development of adult polycystic kidney disease. *Hum Mol Genet* 18: 2523–2531, 2009
56. Zhou J: Polycystins and primary cilia: primers for cell cycle progression. *Annu Rev Physiol* 71: 83–113, 2009
57. Happé H, Leonhard WN, van der Wal A, van de Water B, Lantinga-van Leeuwen IS, Breuning MH, de Heer E, Peters DJ: Toxic tubular injury in kidneys from Pkd1-deletion mice accelerates cystogenesis accompanied by dysregulated planar cell polarity and canonical Wnt signaling pathways. *Hum Mol Genet* 18: 2532–2542, 2009
58. Bastos AP, Piontek K, Silva AM, Martini D, Menezes LF, Fonseca JM, Fonseca II, Germino GG, Onuchic LF: Pkd1 haploinsufficiency increases renal damage and induces microcyst formation following ischemia/reperfusion. *J Am Soc Nephrol* 20: 2389–2402, 2009
59. Weimbs T: Third-hit signaling in renal cyst formation. *J Am Soc Nephrol* 22: 793–795, 2011
60. Ong AC, Harris PC: Molecular pathogenesis of ADPKD: the polycystin complex gets complex. *Kidney Int* 67: 1234–1247, 2005
61. Harris PC, Rossetti S: Determinants of renal disease variability in ADPKD. *Adv Chronic Kidney Dis* 17: 131–139, 2010
62. Harris PC, Torres VE: Polycystic kidney disease. *Annu Rev Med* 60: 321–337, 2009

63. Grantham JJ: Rationale for early treatment of polycystic kidney disease. *Pediatr Nephrol* 30: 1053–1062, 2015
64. Shillingford JM, Murcia NS, Larson CH, Low SH, Hedgepeth R, Brown N, Flask CA, Novick AC, Goldfarb DA, Kramer-Zucker A, Walz G, Piontek KB, Germino GG, Weimbs T: The mTOR pathway is regulated by polycystin-1, and its inhibition reverses renal cystogenesis in polycystic kidney disease. *Proc Natl Acad Sci U S A* 103: 5466–5471, 2006
65. Shillingford JM, Piontek KB, Germino GG, Weimbs T: Rapamycin ameliorates PKD resulting from conditional inactivation of Pkd1. *J Am Soc Nephrol* 21: 489–497, 2010
66. Tao Y, Kim J, Schrier RW, Edelstein CL: Rapamycin markedly slows disease progression in a rat model of polycystic kidney disease. *J Am Soc Nephrol* 16: 46–51, 2005
67. Wahl PR, Serra AL, Le Hir M, Molle KD, Hall MN, Wüthrich RP: Inhibition of mTOR with sirolimus slows disease progression in Han:SPRD rats with autosomal dominant polycystic kidney disease (ADPKD). *Nephrol Dial Transplant* 21: 598–604, 2006
68. Wu M, Wahl PR, Le Hir M, Wackerle-Men Y, Wuthrich RP, Serra AL: Everolimus retards cyst growth and preserves kidney function in a rodent model for polycystic kidney disease. *Kidney Blood Press Res* 30: 253–259, 2007
69. Berthier CC, Wahl PR, Le Hir M, Marti HP, Wagner U, Rehrauer H, Wüthrich RP, Serra AL: Sirolimus ameliorates the enhanced expression of metalloproteinases in a rat model of autosomal dominant polycystic kidney disease. *Nephrol Dial Transplant* 23: 880–889, 2008
70. Shillingford JM, Leamon CP, Vlahov IR, Weimbs T: Folate-conjugated rapamycin slows progression of polycystic kidney disease. *J Am Soc Nephrol* 23: 1674–1681, 2012
71. Armour EA, Carson RP, Ess KC: Cystogenesis and elongated primary cilia in Tsc1-deficient distal convoluted tubules. *Am J Physiol Renal Physiol* 303: F584–F592, 2012
72. Chen J, Chen JK, Nagai K, Plieth D, Tan M, Lee TC, Threadgill DW, Neilson EG, Harris RC: EGFR signaling promotes TGFβ-dependent renal fibrosis. *J Am Soc Nephrol* 23: 215–224, 2012
73. Chen J, Chen JK, Conway EM, Harris RC: Survivin mediates renal proximal tubule recovery from AKI. *J Am Soc Nephrol* 24: 2023–2033, 2013
74. Chen J, Chen MX, Fogo AB, Harris RC, Chen JK: mVps34 deletion in podocytes causes glomerulosclerosis by disrupting intracellular vesicle trafficking. *J Am Soc Nephrol* 24: 198–207, 2013
75. Chen JK, Falck JR, Reddy KM, Capdevila J, Harris RC: Epoxyeicosatrienoic acids and their sulfonimide derivatives stimulate tyrosine phosphorylation and induce mitogenesis in renal epithelial cells. *J Biol Chem* 273: 29254–29261, 1998

This article contains supplemental material online at http://jasn.asnjournals.org/lookup/suppl/doi:10.1681/ASN.2014121264/-/DCSupplemental.